Modeling and Simulation of Semibatch Emulsion Polymerization

BOGENG LI* and BRIAN W. BROOKS†

Department of Chemical Engineering, Loughborough University of Technology, Loughborough, Leicestershire, LE11 3TU, United Kingdom

SYNOPSIS

By taking advantage of recent theoretical developments in emulsion polymerization and radical polymerization kinetics at high conversion, a model is developed for simulating seeded semibatch emulsion polymerization. The model is used to calculate the time evolution of the polymerization rate, the monomer conversion, the instantaneous degree of polymerization, the monomer concentration in particles, the average radical number per particle, and the propagation rate coefficient and termination rate coefficient over the whole course of the polymerization. Experimental observations by previous workers, including the existence of steady-state phenomenon and the broad distributions of molecular weight, are reproduced in the results of the simulation. The gel effect on emulsion polymerization and the open-loop stability of the semibatch process are discussed. © 1993 John Wiley & Sons, Inc.

INTRODUCTION

In emulsion polymerization, semibatch techniques usually offer more flexibility than do batch or continuous techniques. High-value polymer latices with special particle morphology, composition, and other precise characteristics can be tailor-made by adjusting the feed rates of monomer and other ingredients. Also, the polymerization reaction rate and the reaction exotherm can both be manipulated with advantage. Considerable effort has been devoted to both experimental study and mathematical modeling of the semibatch process.[1] Although substantial progress has been made in recent years, further work is required.

For seeded semibatch emulsion polymerization, many workers have observed experimentally that a steady state will be reached during the process if the monomer feed rate is so slow that the reactor is in a starved state with respect to the monomer. In the steady state, the polymerization rate is constant and dependent on the monomer feed rate. By mathematical modeling, Wessling[2] and, recently, Dimitratos et al.[3] studied the relationship between polymerization rate and monomer feed rate under the steady state. In their models, both monomer concentration and radical concentration (or number) in the particles are assumed to be constant in the steady state. Makgawinata et al.[4,5] found that no steady state existed in their system even though the reactor was seeded and the reactions occurred in monomer-starved conditions. For unseeded polymerization, Snuparek[6] obtained steady values for reaction rate and particle number although oscillation phenomena were observed before the steady state was reached. Oscillation in monomer concentration in the particles has also been found by Donescu et al.[7]

Models for semibatch emulsion have also been developed for the monomer feed policy to achieve uniform copolymer composition[8,9] and for process control.[10,11] Overall values for the polymerization rate, the copolymer composition, and the average molecular weight during the polymerization process were predicted by these models.

The present work uses more recent theories of radical number in particles and of radical diffusion-

* Current address: Department of Chemical Engineering, Zhejiang University, Hangzhou 310027, People's Republic of China.

† To whom correspondence should be addressed.

Journal of Applied Polymer Science, Vol. 48, 1811–1823 (1993)
© 1993 John Wiley & Sons, Inc. CCC 0021-8995/93/101811-13

control kinetics. These are incorporated with material and energy balances to develop a computer-based model for improved simulation of dynamic behavior of the semibatch emulsion polymerization. Values are computed for the polymerization rate (and/or the monomer conversion), the degree of polymerization, monomer concentration in particles, the radical number per particle, and kinetic parameters over the whole course of polymerization including the stage after monomer feed ends. Unlike previous work, full allowance is made for the effect of operation parameters on the approach to the steady state, the decay of the polymerization rate, and the gel effect on the emulsion polymerization. The open-loop stability of the semibatch emulsion polymerization reactor is explored. This work is limited to the seeded homogeneous polymerization of water-insoluble monomer with neat monomer feed. An analogous model for simulation of the unseeded copolymerization of water-soluble monomers will be developed subsequently.

MATHEMATICAL MODELS

Reaction Model Assumed

For the emulsion polymerization considered in this work, the following assumptions are made:

1. The monomer feed rate is so slow that the reactor is in a monomer-starved state and no monomer droplets exist.
2. The monomer is sparingly soluble in water and the mass transfer of the monomer to the particles is much faster than the reaction rate, i.e., all the supplied monomer diffuses almost instantaneously into the polymer particle phase.
3. The total number of polymer particles, N_t, does not vary with time, i.e., there is no nucleation of new particles and no agglomeration of particles during the polymerization. All particles are the same size.

Most models presented by previous workers have assumed constant values for the kinetic parameters (such as rate coefficients for propagation and termination) and for the radical concentration in particles. However, in semibatch emulsion polymerization, the monomer concentration in the latex particles is usually much lower than is the monomer concentration in the batch, or continuous-flow, emulsion polymerization because the system is in a monomer-starved state. Therefore, gel effects on termination (and even on propagation) cannot be neglected. This observation is especially important during the initial stage when a seed latex with high monomer conversion is present and during the final stage when the monomer feed has finished.

These considerations led us to construct a new dynamic model that incorporates material and energy balances together with a time-dependent Smith–Ewart recursion differential equation[12] (to determine the radical number per particle) and the diffusion-control theory developed by Soh and Sundberg[13] for kinetic parameters. A detailed description appears in the following sections.

Balances of Material and Energy

The balances for monomer and energy in the semibatch reactor can be derived as follows:

$$\frac{d}{dt}(V_p[M^p]) = F_m - V_R R_p \tag{1}$$

$$\frac{d}{dt}\{V_R \rho_R Cp_R(T_i - T^{(0)})\} = F_m MW_m Cp_m(T_i - T^{(0)}) + (-\Delta H_p)R_p V_R - U_j A_j(T - T_j) \tag{2}$$

where the time-differentials for particle volume, V_p, and total latex volume, V_R, are given by

$$\frac{dV_R}{dt} = \frac{dV_p}{dt} = F_m \frac{MW_m}{\rho_m} + R_p V_R\left(\frac{MW_m}{\rho_p} - \frac{MW_m}{\rho_m}\right) \tag{3}$$

The polymerization rate per unit volume of latex is given by

$$R_p = k_p \bar{n}[M^p]\left(\frac{N_t}{V_R}\right)\Big/ N_A \tag{4}$$

where k_p is the propagation rate constant; $\bar{n}$, the average radical number per particle; $[M^p]$, the monomer concentration in particles; N_t, the total particle number in the reactor; and N_A, the Avogadro's constant.

In eqs. (1)–(3), F_m is the monomer feed rate; MW, the molecular weight; ρ, the density; and Cp, the heat capacity. Subscripts m, p, and R denote monomer, polymer, and total latex, respectively.

$(-\Delta H_p)$ is the heat of polymerization reaction; A, the heat transfer area; U, the heat transfer coefficient, and T, the temperature. Subscripts i and j denote the inlet flux and the jacket, respectively. $T^{(0)}$ is the standard temperature.

For an isothermal system, eq. (2) is not required. In this work, eq. (2) is used to investigate the open-loop stability (i.e., reactor runaway) of the nonisothermal system with constant jacket temperature.

Recursion Differential Equations for Emulsion Polymerization

For a fixed number of polymer particles, the time-dependent Smith–Ewart differential recursion equations are given by[14]

$$\frac{dN_i}{dt} = (N_{i-1} - N_i)\sigma + [(i+1)N_{i+1} - iN_i]k + [(i+2)(i+1)N_{i+2} - i(i-1)N_i]k_t/\nu \quad (5)$$

where N_i is the number of particles that contain i radicals; σ, the average rate for radical entry into a single particle; k, the rate coefficient for radical exit from particles; k_t, the rate coefficient for radical bimolecular mutual termination; and ν, the volume of a single particle. The average number of radicals per particle, $\bar{n}$, is given by

$$\bar{n} = \sum_{i=1}^{\infty} iN_i \Big/ \sum_{i=0}^{\infty} N_i \quad (6)$$

To obtain the value of $\bar{n}$, it is necessary to determine the parameters σ, k, and k_t and to solve the recursion differential eqs. (5). The average rate of radical entry into a single particle, taken from Ref. 15, is expressed as

$$\sigma = k_a[R]_w \quad (7)$$

where $[R]_w$ is the radical concentration in the aqueous phase and the rate coefficient k_a is given by

$$k_a = 2\pi D_w d_p N_A F \quad (8)$$

Here, D_w is the diffusion coefficient for the radicals in the aqueous phase; d_p, the average diameter of a single particle; and F, the radical capture efficiency (which depends on all the resistances to the radical entry other than diffusion).

$[R]_w$ is obtained by solving the following balance equation for the radicals in the aqueous phase:

$$\frac{d[R]_w}{dt} = 2fkd_d[I] + k\bar{n}\left(\frac{N_t}{V_w}\right)\Big/ N_A - k_a[R]_w\left(\frac{N_t}{V_w}\right)\Big/ N_A - k_{tw}[R]_w^2 \quad (9)$$

$[I]$ is the initiator concentration in the aqueous phase, and k_{tw}, the termination rate coefficient in the aqueous phase. Using the steady-state assumption for the aqueous phase, the left-hand side of eq. (9) is assumed to be 0.

The radical desorption rate coefficient can be obtained from Nomura's treatment[16]:

$$k = k_{fm}[M^p]\frac{K_0}{K_0\bar{n} + k_p[M^p]} \quad (10)$$

where k_{fm} is the rate coefficient for chain transfer to the monomer and K_0 is the desorption rate constant for monomer radicals given by

$$K_0 = \frac{12D_w/m_d d_p^2}{1 + 2D_w/m_d D_p} \quad (11)$$

Here, D_p is the diffusion coefficient for the monomer radicals in the particle phase, and m_d, the partition coefficient for the monomer radicals between particles and the aqueous phase. k_t in eq. (5) should be evaluated by the diffusion-control theory. A detailed description is given in the next section.

Considerable progress has been made in obtaining solutions to the recursion differential eqs. (5),[17] but, until now, it has not proved possible to obtain an entirely general solution. Numerical solutions are available for reaction systems in which the radical termination in particles is quite fast so that the number of particles containing j or more radicals can be neglected (j is usually assumed to be two or three). However, for systems in which the termination is limited by diffusion of radical chains, the method usually gives a value for the radical number per particle that is too small. Some approximate analytical solutions have been obtained under certain circumstances. When the rate of radical termination in the particles is not high enough for it to be the dominant radical-loss mechanism and when the parameters σ, k, and k_t/ν are constant, Birtwistle and Blackley[18] gave

$$\bar{n} = 2\sigma\frac{\tanh(at/2)}{a + k\tanh(at/2)} \quad (12)$$

where $a = (4\sigma k_t/\nu + k^2)^{1/2}$. For the case in which

radical loss is predominantly by termination, the values calculated by eq. (12) are too low.[19]

On the other hand, Birtwistle and Blackley[18] retreated the "two-state" model of Lichti et al.[20] for the case in which the number of particles containing three or more radicals was zero and the number containing two radicals is very small and stationary. They gave

$$\bar{n} = \frac{\sigma}{\sigma + q}\{1 - \exp[-(\sigma + q)t]\} \qquad (13)$$

where $q = k + \sigma(k_t/\nu)/[k + (k_t/\nu)]$; parameters σ, k, and k_t/ν are also constant. However, for cases covered by the first solution, eq. (13) gives low values.

As mentioned above, the rate coefficient of radical termination in particles, k_t, will change with the varying of monomer concentration in particles as the polymerization proceeds (at least during the stages before reaching steady state and after ending monomer feed). The possibility of diffusion affecting σ and k also exists. It appears that no one solution can be used to treat the whole course of the process. However, a new treatment of Li and Brooks[21] produced an expression for predicting changes in $\bar{n}$ that gives accurate results over a wide range of conditions. This expression will be used here and takes the form

$$\frac{d\bar{n}}{dt} = \sigma - k\bar{n} - f(k_t/\nu)\bar{n}^2 \qquad (14)$$

where

$$f = \frac{2(2\sigma + k)}{2\sigma + k + (k_t/\nu)} \qquad (15)$$

A Runge–Kutta algorithm is used to solve the differential eq. (14) together with the differential eqs. (1)–(3).

Diffusion-control Model of Kinetic Parameters

A complete model of the gel effect should describe continuous changes in k_p, k_t, and other kinetic parameters (such as chain transfer constant) throughout the whole polymerization from low conversion of monomer through the intermediate conversion to very high conversion. To simulate the semibatch process over whole course of the reaction, a relatively complete gel effect model is necessary. However, many existing theoretical or semiempirical models are limited to particular ranges of conversion. In a series of papers, Soh and Sundberg[13] combined the free volume and the entanglement concepts and developed a relatively comprehensive model for treating the kinetics of bulk polymerization over the whole conversion range. Four phases (intervals) with respect to the conversion curve were defined. Different treatment for each phase, with smooth transitions between them, was presented. A good fit to bulk polymerization data for six different monomers has been given. Using ESR measurement to determine $\bar{n}$, Ballard et al.[22] demonstrated that k_p for seeded emulsion polymerization can be adequately described by the Soh and Sundberg model.

In this work, we use the Soh and Sundberg model to treat both the propagation and the termination coefficients in particles. According to Soh and Sundberg,[13c] k_p at high conversion can be written in term of two limiting rate coefficients:

$$1/k_p = 1/k_{p0} + 1/k_{pvf} \qquad (16)$$

where k_{p0} corresponds to the rate coefficient in the absence of diffusion control and k_{pvf} is its value when there is absolute diffusion control, which is given by the Rabinowich-type expression

$$k_{pvf} = 3.4 \times 10^{15} D_m/M_0^{1/3} \qquad (17)$$

where D_m is the diffusion coefficient for monomer and M_0 is the molar concentration of pure monomer; the units of (cm^2/s) and (mol/L) are used for D_m and M_0, respectively.

In this work, D_p in eq. (11) is assumed to be equal to D_m because the monomer molecule and monomer radical have similar sizes. Following the theory of Fujita,[23]

$$D_m/kT = 1/\zeta_m \qquad (18)$$

where k is Boltzmann's constant and ζ_m is the friction coefficient given by

$$\zeta_m = (\zeta_s)_{\nu fp}\exp(1/\nu_f - 1/\nu_{fp}) \qquad (19)$$

Here, ν_f is the free volume of the polymer–monomer system (i.e., monomer-swollen polymer particles in this work), given by

$$\nu_f = \nu_{fm}\phi_m + (1 - \phi_m)\nu_{fp} \qquad (20)$$

ν_{fm} and ν_{fp} are the free-volume contributions from monomer and polymer. $(\zeta_s)_{\nu fp}$ in eq. (19) is the friction coefficient at the reaction temperature. All these

parameters can be obtained following the literature.[13]

Calculation of k_t is more difficult. Following Soh and Sundberg,[13d] in Phase I (i.e., low conversion region), $k_t = k_{t0}$, where k_{t0} is the rate coefficient in the absence of diffusion control. In Phase II (i.e., high-conversion region),

$$k_t = k_{tvf} Z \tag{21}$$

$$k_{tvf} = (k_{t0}/Z|_{\nu_f=\nu_{fxc}}) \exp(1/\nu_{fxc} - 1/\nu_f) \tag{22}$$

where ν_{fxc} is the free volume at the onset of the gel effect. Z is the dimensionless parameter that is a function of two special parameters β and γ:

$$\beta = x_c C_m \tag{23}$$

$$\gamma = x_c (R_i k_{tvf})^{1/2}/k_p[M] \tag{24}$$

Soh and Sundberg[13a] gave a master curve for values of Z. From this curve, we find that Z is given by the expression

$$Z = 1 - \exp(-1.8\beta - 1.25\gamma\sqrt{Z}) \tag{25}$$

This expression will be used to give values of Z in the present work. The initiation rate, R_i, and the monomer concentration, $[M]$, are replaced by the radical entry rate into particles and the monomer concentration in particles.

The critical degree of polymerization for entanglement in a polymer–monomer mixture, x_c, is given by

$$x_c = x_{c0}/(1 - \phi_m) \tag{26}$$

where x_{c0} is the x_c value for pure polymer.

In Phases III and IV (the very high conversion region), Soh and Sundberg's model allowed for the occurrence of the termination reaction even when the polymer radical is completely immobile. Thus,

$$k_t = (k_{tvf} + k_{tp})Z \tag{27}$$

where Z is a function of parameters β, γ, and W. W is defined as

$$W = k_{tvf}/(k_{tvf} + k_{tp}) \tag{28}$$

The residual termination rate coefficient, k_{tp}, is given by

$$k_{tp} = \pi\delta^2 a N_A k_p[M] f_t/(1000 j_c^{1/2}) \tag{29}$$

where δ is the collision radius for the termination sphere; a, the average root-mean-square length per monomer unit; f_t, the efficiency factor; and j_c, the entanglement spacing. Values for all these entities can be determined by the methods presented in Ref. 13b. A trial-and-error solution is required for obtaining values of Z, W, and k_{tp}.

NUMERICAL IMPLEMENTATION

The differential and algebraic equations given in the previous sections were solved numerically using a Runge–Kutta algorithm. Iterative or trial-and-error methods were used in calculating some intermediate parameters such as Z and W. A computer program was written to describe the seeded homopolymerization of styrene, a typical water-insoluble monomer. In this work, values of parameters were obtained from the literature, as shown in Table I. Polymerization rate, monomer concentration in the particles, average radical number per particle, radical concentration in the particles, kinetic parameters (k_p, k_t, and k_{fm}), and physical parameters (σ and k) were obtained as function of time. Values for instantaneous conversion, overall conversion, and instantaneous number-average degree of polymerization were also calculated by using the following equations.

The instantaneous conversion (the ratio of the amount of polymer in the reactor to the total amount

Table I Values of the Physical and Chemical Parameters Used in Calculations

$\rho_m = 923.6 - 0.887t^0$ (g/dm^3)[24]	
$\rho_p = 1050.1 - 0.621t^0$ (g/dm^3)[25]	
$Cp_m = 1.6262 + 3.124 \times 10^{-3}T$ (kJ/kg K)[24]	
$Cp_p = 1.1425 + 4.885 \times 10^{-3}T$ (kJ/kg K)[25]	
$\nu_{fxc} = 1.111 \exp(-788.51/T)$[13d]	
$\nu_{fm} = 0.112 + 6.2 \times 10^{-4}t^0$ [13c]	
$k_d = 4.5 \times 10^{16}\exp(-140{,}200/RT)$[25]	
$k_{p_0} = 2.17 \times 10^7\exp(-3{,}905/T)$[13d]	
$k_{tw} = k_{t_0} = 8.2 \times 10^9\exp(-1{,}747/T)$[13d]	
$F = 1 \times 10^{-3}$ [15]	
$D_w = 10^{-6}$ (cm^2/sec)[15]	
$m_d = 1600$[26]	
$x_c = 385$[27]	
$a = 7.4 \times 10^{-8}$ (cm)[27]	
$\nu_{fp} = 0.0245 + 4.5 \times 10^{-4}(t^0 - 82)$	$t \geq 82$[13c]
$\nu_{fp} = 0.0245 + 1.4 \times 10^{-4}(t^0 - 82)$	$t < 82$[13c]
$C_{m_0} = 1.0 \exp(-3{,}212/T)$[25]	
$C_m = C_m k_p/k_{p0}$	
$(-\Delta H_p) = 69.9$ (kJ/mol)[25]	
$f = 0.7$	

of polymer and monomer in the reactor at time t, i.e., weight fraction of polymer in particle) is given by

$$x = (1 - [M^p]MW_m/\rho_{p-m}) \times 100\% \quad (30)$$

(It is assumed that the monomer is sparingly soluble in water.)

The overall conversion (the ratio of the amount of polymer in the reactor to the total amount of polymer and monomer in the recipe) is given by

$$X = xf_m \quad (31)$$

where ρ_{p-m} is the density of the monomer-swollen particle and f_m is the monomer feed fraction. The instantaneous number-average degree of polymerization is given by

$$\bar{x}_n = R/(R_t/2 + R_{trm}) \quad (32)$$

where R, R_t, and R_{trm} are polymerization rate, termination rate, and chain transfer rate to monomer, respectively. Their units are all in mol/s, i.e.,

$$R = R_p V_R \quad (33)$$

$$R_t = k_t(N_t\bar{n}/V_pN_A)^2V_p \quad (34)$$

and

$$R_{trm} = k_{fm}\bar{n}[M^p]N_t/N_A \quad (35)$$

The recipes and operation conditions that were assumed to apply are given in Table II. The relationship between the operation variables and changes in the dependent variables was investigated.

RESULTS AND DISCUSSION

Figure 1 shows the polymerization rate curve as a function of time at different monomer feed rates.

Table II Recipes and Operation Conditions Used in Calculations

Monomer: 500 mL
  Initial charge for preparing seed latex: 5–15%
    (in most cases, 10%, which gives $\nu = 5 \times 10^{-20}$ dm^3)
Water: 500 mL
  Aqueous solution containing KPS: 0.04 mol
Temperature: 50°C
Particle number: 5×10^{17}–2×10^{18}/L-latex
Monomer feed rate: 1×10^{-4}–1.2×10^{-3} mol/s

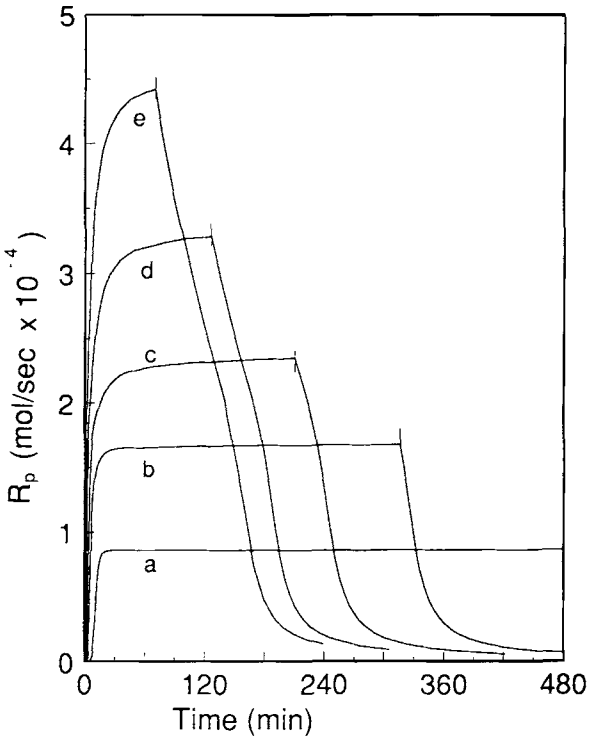

Figure 1 Polymerization rate as a function of time at various monomer feed rates when $N_t = 1 \times 10^{18}$ and $T = 50$°C: (a) $F_m = 1.0 \times 10^{-4}$ mol s^{-1}; (b) $F_m = 2.0 \times 10^{-4}$ mol s^{-1}; (c) $F_m = 3.0 \times 10^{-4}$ mol s^{-1}; (d) $F_m = 5.0 \times 10^{-4}$ mol s^{-1}; (e) $F_m = 9.0 \times 10^{-4}$ mol s^{-1}. The vertical bar denotes the end point for monomer feed.

When the monomer feed rate is low, it can be seen that the reaction rate rises initially and then reaches a steady state. The lower the monomer feed rate, the faster the system reaches the steady state. When the feed rate is relatively high, the steady state is unlikely to occur even though the system is still in a monomer-starved state. These results are in agreement with the experimental observations by previous workers.[6] Rapid decay of the polymerization after the end of the monomer feed was also found. The reaction rates drop from the different steady-state values to a common very low value; this is not zero because there is the same small quantity of residual monomer (i.e., there is limited conversion). The overall conversions as a function of time are shown in Figure 2. Before the monomer feed ends, a linear relationship between the conversion and time is found. A limited conversion is obtained; this is the same for different monomer feed rates because the polymerization temperature is the same.

Figure 3(a) and (b) shows the change of instantaneous number-average polymerization degree with

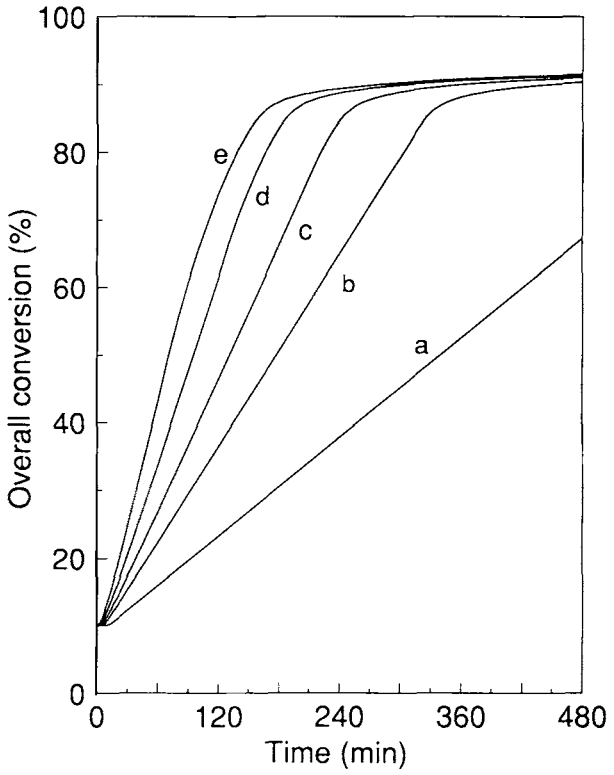

Figure 2 Overall conversion as a function of time at various monomer feed rates. Conditions and curves as for Figure 1.

time. It is found that the degree of polymerization always increases during the monomer feed stage even though the reactor has reached the steady state in which the monomer concentration in the particles and the average radical number per particle are constant (as shown in Figs. 4 and 5). This is attributed mainly to the expansion of particle volume with time during the monomer feed period. As the volume expands, both the radical concentration in particles and the termination rate decrease. This result leads us to expect that the polymer formed by the semibatch process has a relatively broad molecular weight distribution (chain transfer to monomer is not predominant in this case). The other important factor that affects the degree of polymerization is the monomer concentration in particles. As shown in Figure 4, a lower monomer feed rate always gives lower monomer concentration in particles. When the monomer concentration is so low that the radical loss in particles is predominantly by the radical exit from the particles, an increase in the monomer feed rate will lead to an increase in the degree of polymerization, as shown in Figure 3(a). However, when the monomer concentration is already high enough for the radical loss to be predominantly by termination, the gel effect on the termination still exists. Then, an increase in monomer concentration is likely to increase the rate of the radical termination and the degree of polymerization will decrease, as shown in Figure 3(b). When the conversion reaches about 85%, the degree of polymerization is found to decrease sharply and a common decay curve is followed for the different monomer feed rates.

Figure 4 shows the monomer concentration in particles as a function of the monomer feed fraction at various monomer feed rates. Figure 5 shows variation of the radical concentration in particles and the average radical number per particle during the polymerization. These results confirmed the assumption presented by Wessling[2] and Dimitratos et al.[3] that the monomer concentration in particles and the average number of radicles per particle are almost constant in the steady state.

Figure 6 shows the changes of k_p, k_t, and $\bar{n}$ with the fraction of polymer in the monomer-swollen particle. It has been found that the average number of radicals per particle is nearly unchanged and approximately equal to 0.5 when the fraction of polymer is lower than about 86%, although significant change occurs in the rate coefficient of termination k_t. This is attributed to the compartmentalizing action of the particles in emulsion polymerization. In emulsion polymerization, there seems to be no gel effect on k_p (at low fractions of polymer) because its value is constant. However, the overall gel effect on the molecular weight of the polymer is quite clear according to eq. (32) and as shown in Figure 3.

It has been noticed that k_t is also dependent on the degree of polymerization. The values shown in Figure 6, determined by Soh and Sundberg's model, has taken this into account.

The effects of some operational conditions on the approach to the steady state are shown in Figures 7–9. In addition to the monomer feed rate, shown in Figure 1, the initial particle volume and the conversion of seed latex also have a distinct influence on the approach to the steady state. The time required to reach the steady state is shorter if the initial particle volume is small or if the concentration of monomer in the seed latex is already close to the steady-state value. This suggests that a steady state will be reached more quickly if the seed latex is prepared *in situ*. An increase in particle number will increase the reaction rate, as shown in Figure 7, but does not affect the approach to the steady state if the initial particle volume is the same.

Figure 10(a) shows the relationship between reaction rate in the steady state, R_s, and the monomer

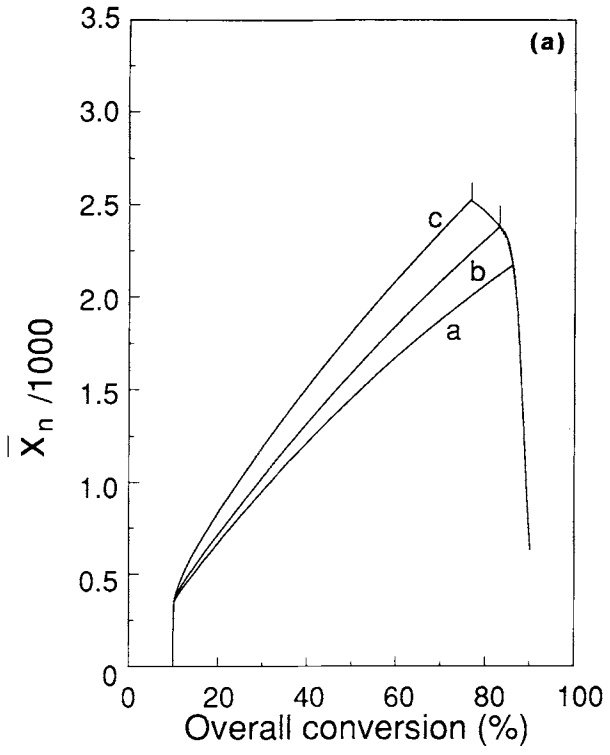

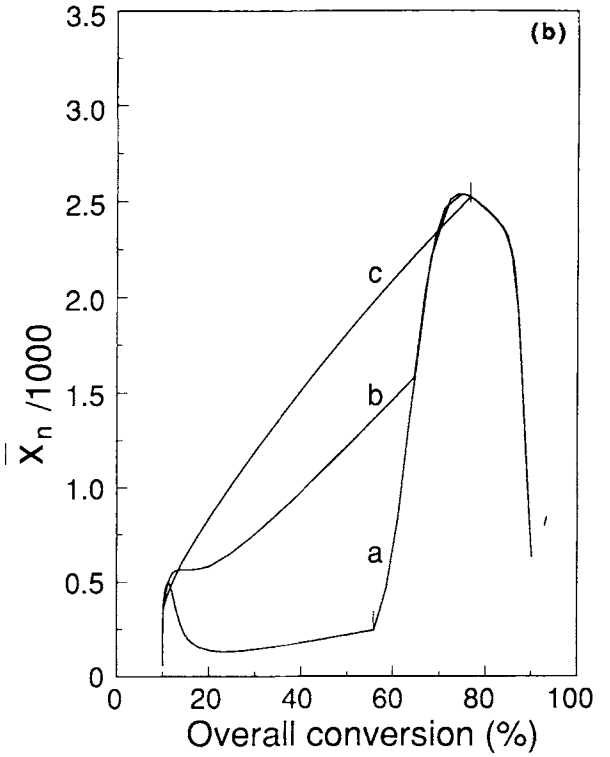

Figure 3 **(a)** Instantaneous number-average degree of polymerization as a function of overall conversion at various monomer feed rates: (a) $F_m = 1.0 \times 10^{-4}$ mol s^{-1}; (b) $F_m = 2.0 \times 10^{-4}$ mol s^{-1}; (c) $F_m = 3.0 \times 10^{-4}$ mol s^{-1}. The vertical bar denotes the end point for monomer feed.

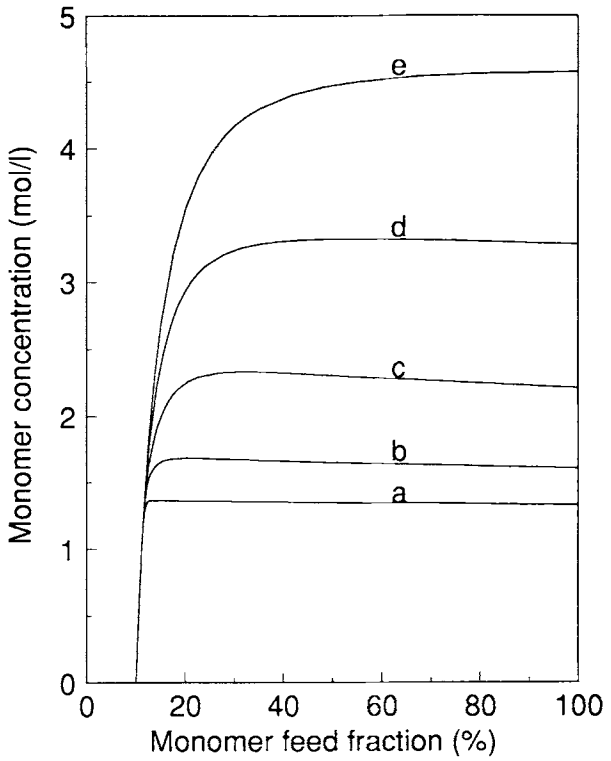

Figure 4 Monomer concentration in the particles as a function of monomer feed fraction. Conditions and curves as for Figure 1.

feed rate, F_m. A good linear relationship is obtained between $1/R_s$ and $1/F_m$ (rather than between R_s and F_m) as shown in Figure 10(b). The result agrees with the equation derived by Wessling[2] and Dimitratos et al.[3]:

$$1/R_s = G + 1/F_m \tag{36}$$

where $G = N_A MW_m/k_p N_t \bar{n} \rho_m$. The larger N_t, the smaller G is.

Figure 11(a) and (b) illustrates the open-loop stability of the semibatch emulsion polymerization reactor. The reactor is assumed to be a stirred tank 1 m^3 in volume and with an unchanged inlet temperature (20°C) and jacket temperature (50°C). The heat transfer coefficient, U_j, is taken as 500 kcal/m^2 h, and $A_j = \pi(4V_R/\pi)^{2/3} = 3.69$ m^2. It is assumed that no feedback control system is used to

(b) Instantaneous number-average degree of polymerization as a function of overall conversion at various monomer feed rates: (a) $F_m = 7.0 \times 10^{-4}$ mol s^{-1}; (b) $F_m = 5.0 \times 10^{-4}$ mol s^{-1}; (c) $F_m = 3.0 \times 10^{-4}$ mol s^{-1}. The vertical bar denotes the end point for monomer feed.

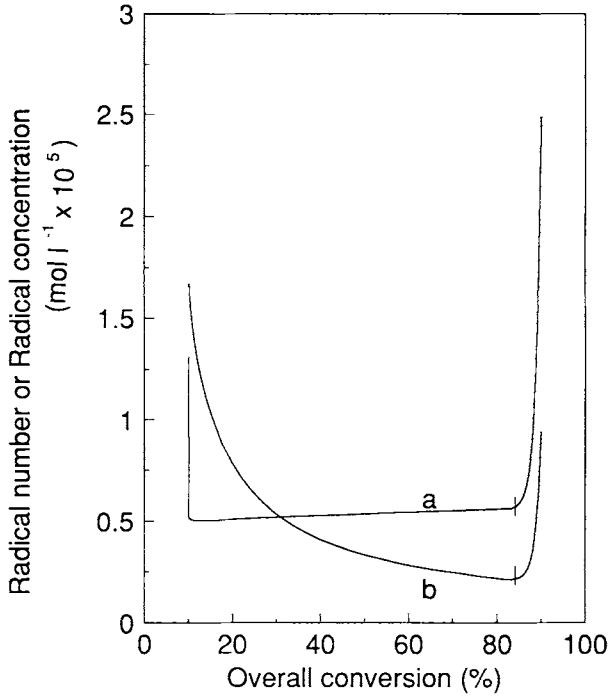

Figure 5 Average radical number ($\bar{n}$) [curve (a)] and radical concentration in the particles [curve (b)] during polymerization when $F_m = 2.0 \times 10^{-4}$. The vertical bar denotes the end point for monomer feed.

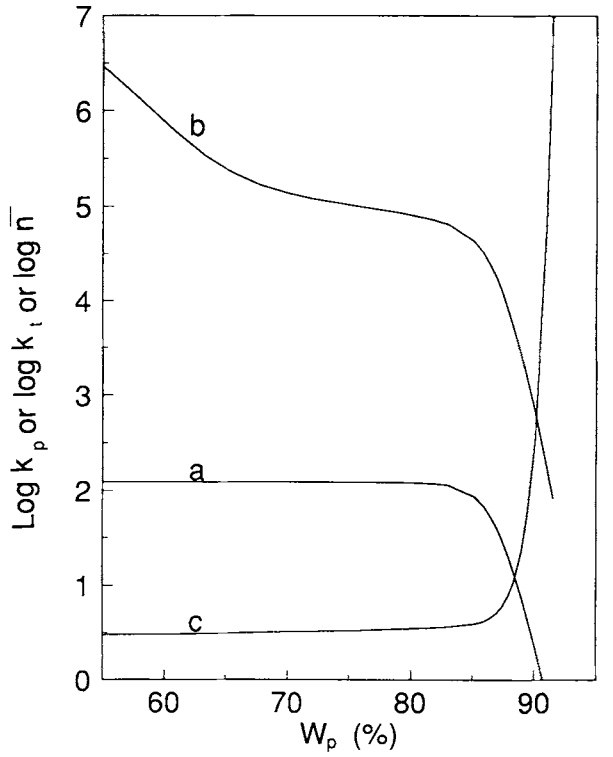

Figure 6 k_p [curve (a)], k_t [curve (b)], and average radical number ($\bar{n}$) [curve (c)] as functions of polymer weight fraction.

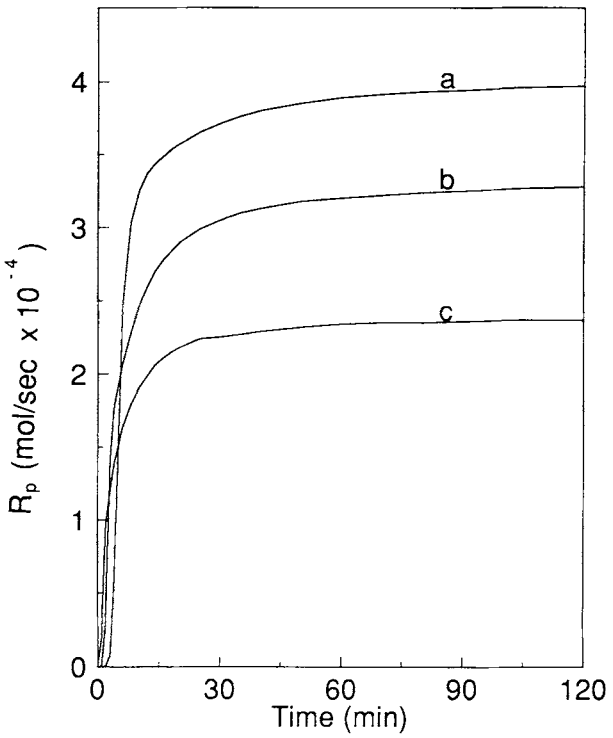

Figure 7 Effect of particle number on the approach to the steady state when $F_m = 5.0 \times 10^{-4}$ and $v = 5 \times 10^{-20}$ dm^3. Curve (a): $N_t = 2.0 \times 10^{18}$; curve (b): $N_t = 1.0 \times 10^{18}$; curve (c): $N_t = 5.0 \times 10^{17}$.

adjust the jacket temperature in response to the resulting error signal. It is found that the system still can reach a steady state when the monomer feed rate is low. When the feed rate is high, both reaction rate and temperature oscillate with time. Converging oscillations (or possibly limit cycles) can be predicted. The convergence value is determined by the monomer feed rate. When the reaction rate is larger than the monomer feed rate, the monomer concentration (and therefore the reaction rate) will decrease. In practice, the monomer feed is likely to be finished before the convergence value is reached. The dotted parts of the curves in Figure 11 show changes in reaction rate and temperature with time that would occur if the monomer feed was continued. These results indicate that the semibatch emulsion polymerization is a open-loop stable process.

CONCLUSIONS

A semibatch emulsion polymerization reactor usually operates in starved state with respect to the monomer. The reaction kinetics and the reactor stability are likely to be different from those found in batch and continuous processes. The model pre-

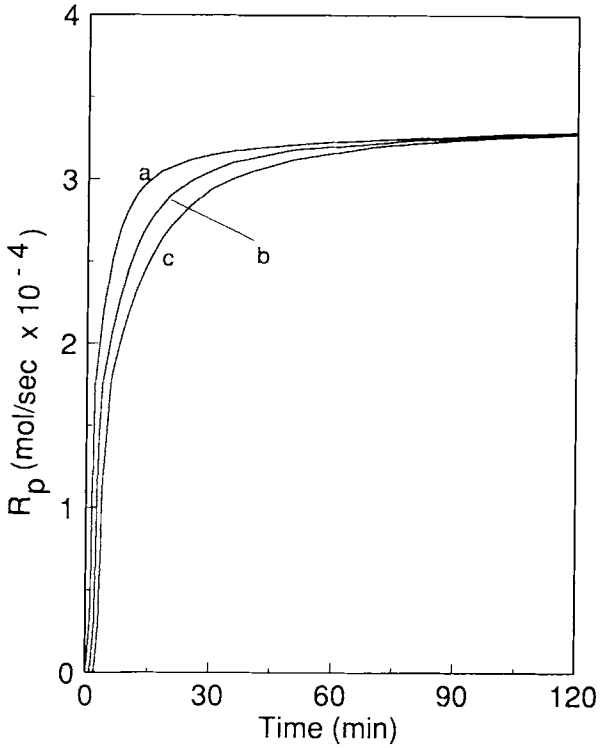

Figure 8 Effect of initial volume of particle phase on the approach to the steady state when $F_m = 5.0 \times 10^{-4}$ and $N_t = 1.0 \times 10^{18}$. Curve (a): initial volume of particle phase 25 mL; curve (b): initial volume of particle phase 50 mL; curve (c): initial volume of particle phase 75 mL.

sented in here is available for treating the seeded semibatch emulsion homopolymerization of a water-insoluble monomer with neat monomer feed. It gives insight into the time evolution of (a) the overall variables such as polymerization rate, monomer conversion, and degree of polymerization, (b) the intrinsic variables such as monomer and radical concentrations in particles, and (c) the physical and chemical parameters such as radical entry and exit rate coefficients and propagation and termination rate coefficients. A wide range of predictions that are internally consistent and compatible with the experimental observations by previous workers is obtained. The results lead to several conclusions:

(i) When the monomer feed rate is relative low, a steady state in the reaction rate can be reached after the start-up period is complete. In the steady state, the relationship between the reaction rate and the monomer feed rate is $1/R_s = G + 1/F_m$. When the monomer feed rate is high, the steady state is unlikely to exist although the reactor still is in a monomer-starved state.

(ii) The monomer concentration and the average radical number per particle are constant in the steady state but the degree of polymerization still changes because the radical concentration in particles (rather than radical number) continues to change. Therefore, a broad distribution of molecular weight might be obtained.

(iii) The monomer concentration in the particles decreases with a decrease in the monomer feed rate. This causes a large decrease in the termination rate coefficient, k_t. However, $\bar{n}$ is nearly unchanged as long as the monomer concentration is not so low that radical loss is predominantly by radical exit. In this case, the propagation rate coefficient, k_p, is also almost unchanged. Therefore, it might be claimed that (from the monomer conversion results) there is no gel effect on the emulsion polymerization. However, a large change in the molecular weight of the polymer may still occur as a result of changes of k_t and radical concentration. The higher the monomer feed rate, the lower the molecular weight. When the monomer feed rate is very

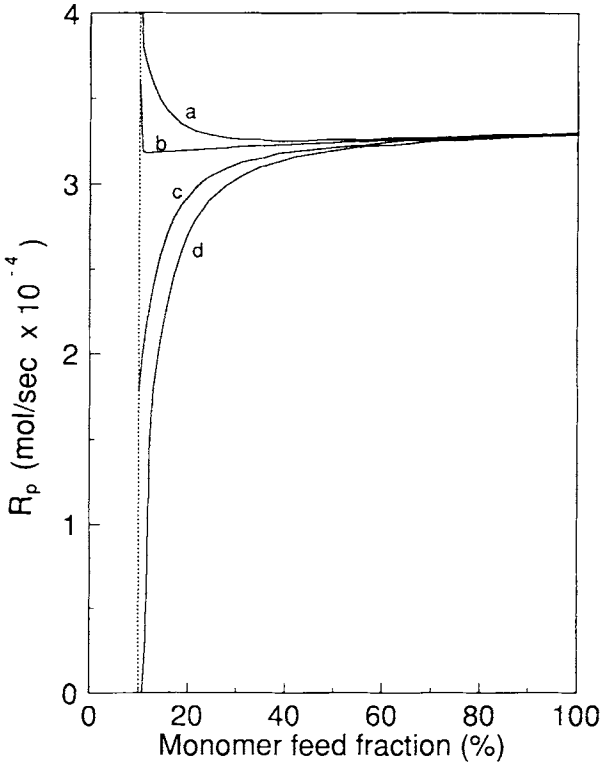

Figure 9 Effect of seed latex conversion on the approach to the steady state. Curve (a) conversion = 50%; curve (b) conversion = 60%; curve (c) conversion = 80%; curve (d) conversion = 100%.

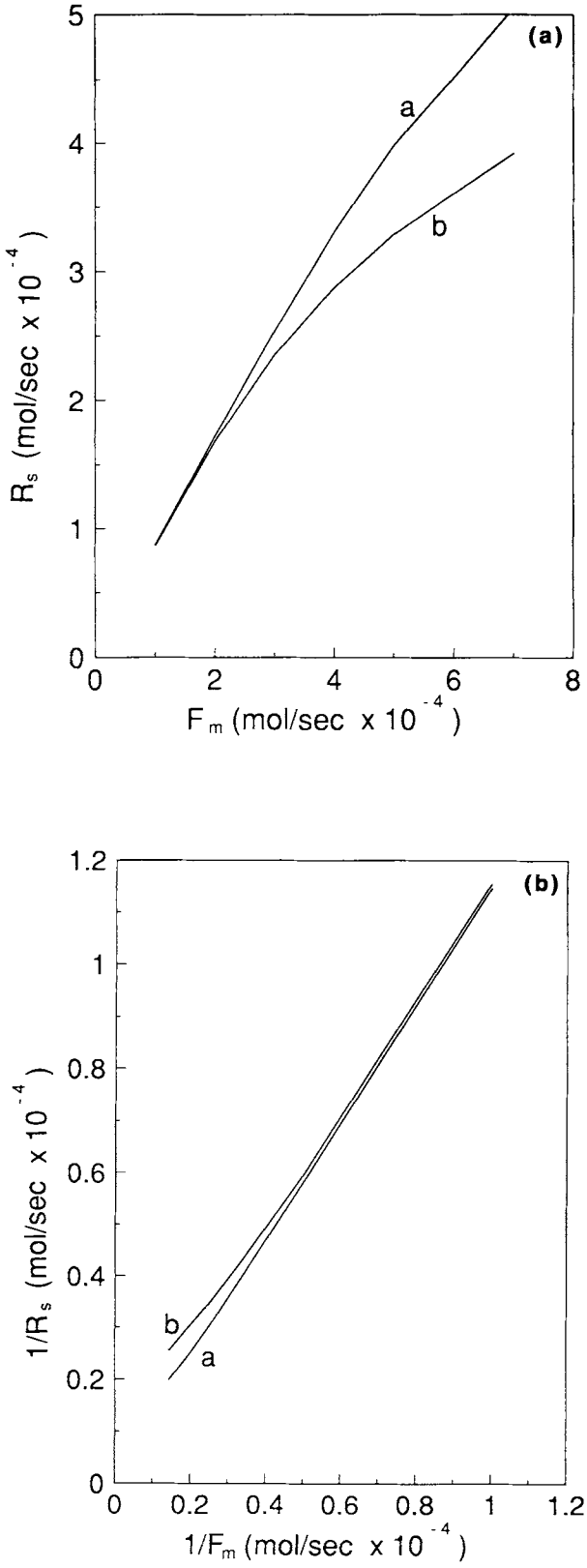

Figure 10 **(a)** The relationship between steady-state polymerization rate (R_s) and monomer feed rate (F_m). Curve (a): $N_t = 2.0 \times 10^{18}$; curve (b): $N_t = 1.0 \times 10^{18}$.

(b) The relationship between $1/R_s$ and $1/F_m$. Curve (a): $N_t = 2.0 \times 10^{18}$; curve (b): $N_t = 1.0 \times 10^{18}$.

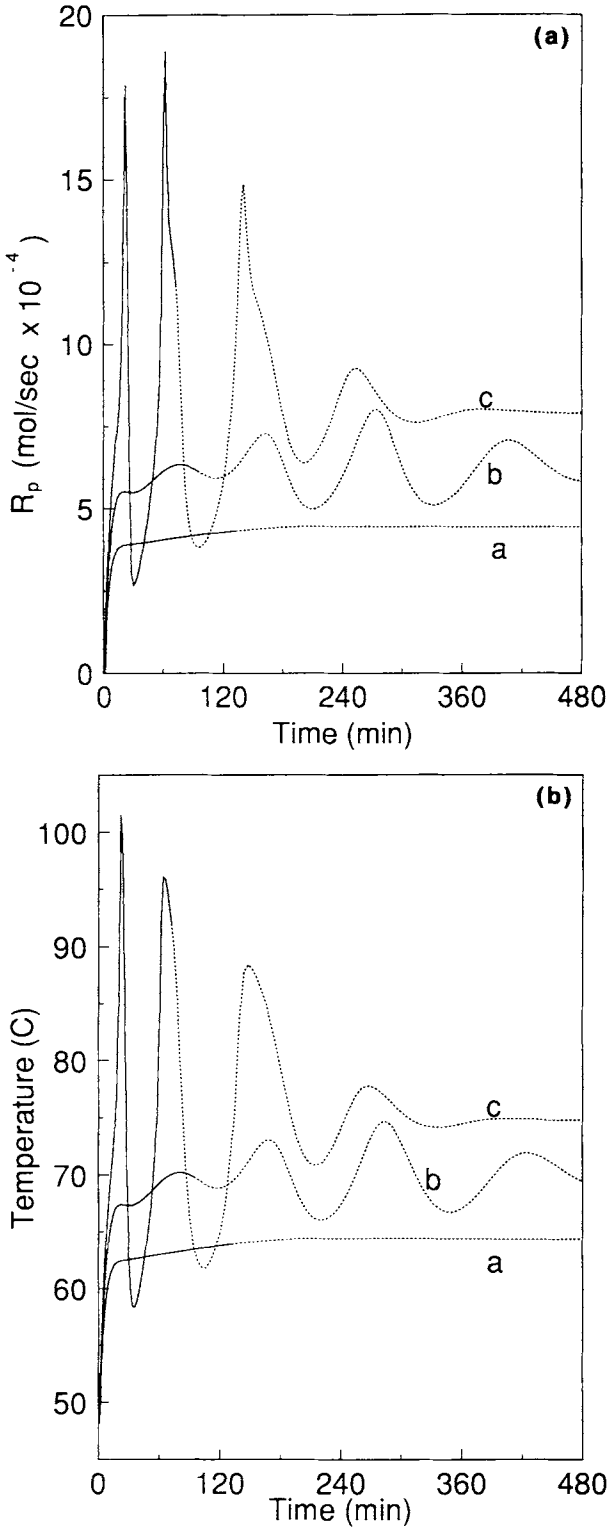

Figure 11 **(a)** The open-loop stability of a semibatch emulsion polymerization reactor. (Reaction rate for different monomer feed rates.) Volume of water = 0.5 m^3; volume of monomer = 0.5 m^3. Curve (a): $F_m = 0.5$ mol s^{-1}; curve (b): $F_m = 0.7$ mol s^{-1}; curve (c): $F_m = 0.9$ mol s^{-1}.

(b) The open-loop stability of a semibatch emulsion polymerization reactor. (Reaction temperature for different monomer feed rates.) Curves as for Figure 11(a).

low, so that the radical loss is dominated by the radical exit from the particles, an increase in monomer feed rate will increase the molecular weight.

(iv) In addition to using a low monomer feed rate, a smaller initial particle volume and an appropriate concentration of monomer in the seed latex can facilitate a rapid approach to the steady state.

(v) The semibatch emulsion polymerization reactor is open-loop stable.

The model is limited to certain circumstances such as the use of seeded systems, neat monomer feed, a water-insoluble monomer, and homopolymerization. To extend the model, some recent developments in the determination of monomer partition (between polymer particles and aqueous phases) and predicting the nucleation of new particles need to be adopted.

NOTATION

A heat transfer area (m^2)
a average root-mean-square length per monomer unit (cm) constant in eq. (12)
C_m chain transfer constant to monomer
Cp heat capacity (kJ/kg K)
D diffusion coefficient (cm^2/s)
d_p average diameter of particle (cm)
F radical capture efficiency
F_m monomer feed rate (mol/s)
f initiator efficiency
f_m monomer feed fraction (%)
f_t efficiency factor for k_{tp}
G constant in eq. (36)
$-\Delta H_p$ heat of polymerization (kJ/mol)
$[I]$ initiator concentration in aqueous phase (mol/dm^3-water)
j_c entanglement spacing
K_0 diffusion rate of a radical out of particle (s^{-1})
k rate coefficient for radical exit from particle (s^{-1})
k_a rate coefficient for radical entry into particle (dm^3/mol s)
k_d rate constant for initiator decomposition (s^{-1})
k_{fm} rate constant for chain transfer to monomer (dm^3/mol s)
k_p rate constant for propagation (dm^3/mol s)
k_{p0} rate constant for propagation in the absence of diffusion control
k_{pvf} rate constant for propagation in the presence of absolute diffusion control
k_t rate constant for termination (dm^3/mol s)
k_{t0} rate constant for termination in the absence of diffusion control
k_{tp} rate constant for the residual termination
k_{tvf} rate constant for the translational termination rate in the unentangled state (dm^3/mol s)
M_0 molar concentration of pure monomer (mol/dm^3)
$[M^p]$ monomer concentration in particles (mol/dm^3)
MW molecular weight
m_d partition coefficient for monomer radicals between particles and aqueous phase
N_A Avogadro's constant
N_i number of particles that contain i radicals
N_t total particle number in the reactor
$\bar{n}$ average radical number per particle
q constant in eq. (13)
R polymerization rate (mol/s)
R_p polymerization rate per unit volume of latex (mol/dm^3-latex s)
$[R]_w$ radical concentration in aqueous phase (mol/dm^3-water)
R_s polymerization rate in the steady state (mol/s)
R_t termination rate (mol/s)
R_{trm} chain transfer rate to monomer (mol/s)
T temperature (K)
t time (s)
t^0 temperature (°C)
U heat transfer coefficient
V volume (dm^3)
v volume of a single particle (dm^3)
v_f free volume
W parameter defined by eq. (28)
X overall conversion defined by eq. (31)
x instantaneous conversion defined by eq. (30)
x_c critical polymerization degree for entanglement
$\bar{x}_n$ instantaneous polymerization degree
Z dimensionless parameter in eqs. (21) and (27)

Greek Symbols

β parameter defined by eq. (23)
γ parameter defined by eq. (24)
δ collision radius for termination sphere (cm)
ζ friction coefficient (dyne s/cm)

ρ density (g/dm^3)
σ average rate of radical entry into a single particle (s^{-1})

Subscripts

m monomer
p polymer or particles
$p - m$ monomer-swollen particles
R latex

REFERENCES

1. B. G. Li and B. W. Brooks, *Polym. Int.*, **29,** 41 (1992).
2. R. A. Wessling, *J. Appl. Polym. Sci.*, **12,** 309 (1968).
3. J. Dimitratos, M. S. El-Aasser, C. Georgakis, and A. Klein, *J. Appl. Polym. Sci.*, **40,** 1005 (1990).
4. T. Makgawinata, PhD Thesis, Lehigh University, 1982; *Diss. Abstr. Int. B,* **42,** 4819 (1982).
5. J. W. Vanderhoff, *J. Polym. Sci. Symp.*, **72,** 161 (1985).
6. J. Snuparek, Jr., *J. Makromol. Chem. Suppl.*, **10/11,** 129 (1985).
7. D. Donescu, K. Gosa, and I. Languri, *Acta Polym.*, **40,** 49 (1989).
8. G. Arzamendi and J. M. Asua, *Makromol. Chem. Macromol. Symp.*, **35/36,** 249 (1990).
9. A. E. Hamielec, J. F. MacGregor, and A. Penlidis, *Makromol. Chem. Macromol. Symp.*, **10/11,** 521 (1987).
10. E. P. Dougherty, *J. Appl. Polym. Sci.*, **32,** 3051, 3079 (1986).
11. J. Dimitratos, C. Georgakis, M. S. El-Aasser, and A. Klein, *Comput. Chem. Eng.*, **13,** 21 (1989).
12. W. V. Smith and R. H. Ewart, *Chem. Phys.*, **16,** 592 (1948).
13. S. K. Soh and D. C. Sundberg, *J. Polym. Sci. Polym. Chem. Ed.*, **20,** (a) 1299; (b) 1315; (c) 1331; (d) 1345 (1982).
14. D. T. Birtwistle and D. C. Blackley, *J. Chem. Soc. Faraday I,* **73,** 1998 (1977).
15. J. M. Asua, V. S. Rodriguez, E. D. Sudol, and M. S. El-Aasser, *J. Polym. Sci. Polym. Chem. Ed.*, **27,** 3569 (1989).
16. M. Nomura, in *Emulsion Polymerisation,* I. Piirma, Ed., Academic Press, New York, 1982, p. 191.
17. B. W. Brooks, *Colloid Polym. Sci.*, **265,** 58 (1987).
18. D. T. Birtwistle and D. C. Blackley, *J. Chem. Soc. Faraday I,* **77,** 413 (1981).
19. B. W. Brooks, *J. Chem. Soc. Faraday I,* **78,** 3137 (1982).
20. G. Lichti, R. G. Gilbert, and D. H. Napper, *J. Polym. Sci. Polym. Chem. Ed.*, **15,** 1957 (1977).
21. B. Li and B. W. Brooks, to appear.
22. M. J. Ballard, R. G. Gilbert, D. H. Napper, P. J. Pomery, P. W. O'Sullivan, and J. H. O'Donnell, *Macromolecules,* **19,** 1303 (1986).
23. H. Fujita and A. Kishimoto, *J. Chem. Phys.*, **34,** 393 (1961).
24. D. H. James, J. B. Gardner, and E. C. Mueller, in *Encyclopedia of Polymerization Science and Technology,* H. F. Mark *et al.*, Eds., Wiley, New York, 1989, Vol. 16, 5.
25. J. Brandrup and E. H. Immergut, Eds., *Polymer Handbook,* 3rd ed., Wiley, New York, 1989.
26. J. M. Asua, E. D. Sudol and M. S. El-Aasser, *J. Polym. Sci. Polym. Chem. Ed.*, **27,** 3903 (1989).
27. J. D. Ferry, *Viscoelastic Properties of Polymers,* 3rd ed., Wiley, New York, 1980.

Received March 18, 1992
Accepted September 16, 1992